Published in final edited form as:
Immunity. 2009 March 20; 30(3): 434–446. doi:10.1016/j.immuni.2008.12.018.

B Lymphocytes Exit Lymph Nodes through Cortical Lymphatic Sinusoids Near to Lymph Node Follicles by a Mechanism Independent of S1P-Mediated Chemotaxis

Rajesh K. Sinha[1,2], **Chung Park**[1,2], **Il-Young Hwang**[1], **Michael D. Davis**[1], and **John H. Kehrl**[1,3]

[1] B-Cell Molecular Immunology Section, Laboratory of Immunoregulation, National Institute of Allergy and Infectious Disease, Bethesda, MD 20892-1888, U.S.A

Abstract

Sphingosine-1 Phosphate (S1P) helps mediate lymphocyte egress from lymph nodes, yet significant mechanistic questions remain. Here we show that B lymphocyte egress sites exist close to lymph node follicles. Recent B cell emigrants localize towards follicle centers, while longer-term residents tend towards cortical sinusoids. Exiting B lymphocytes squeeze through apparent portals in the lymphatic endothelium. Treatment with the S1P receptor agonist FTY720 empties the cortical sinusoids of lymphocytes, blocks lymphatic endothelial penetration, and displaces B lymphocytes into the T cell zone. $S1P_3^{-/-}$ B cells, which lack chemoattractant responses to S1P, transit lymph nodes normally, while *Gnai2*$^{-/-}$ B cells, which have impaired responses to chemokines and S1P, transit more rapidly than do wild type cells. This study identifies a major site of B lymphocyte lymph node egress, shows that FTY720 treatment blocks passage through the cortical lymphatic endothelium, and argues against a functional role for S1P chemotaxis in B lymphocyte egress.

The afferent lymph is low in lymphocytes, whereas the efferent lymph is highly enriched (Hall and Morris, 1965; Young, 1999). This discrepancy arises because peripheral blood lymphocytes enter lymph nodes from the blood, but exit via efferent lymphatics eventually returning to the blood (Gowans, 1957). A great deal of work has been done at the microanatomical level to understand this lymphocyte recirculation. Early light microscopic study of ultra thin sections of rodent lymph nodes revealed an interesting sinus structure termed a “mud stream” that appeared connected downstream to the medullary sinus and extended upstream into the outer cortex (Soderstrom and Stenstrom, 1969). Colloidal carbon injection into afferent lymphatics of the rat mesenteric lymph node revealed connections between the subcapsular, intermediate (cortical), and medullary sinuses (Anderson and Anderson, 1975). The intermediate sinuses formed a lymphatic plexus that surrounded follicles and high endothelial venules (HEVs). Scanning electron microscopy of casts prepared by resin injection of rabbit mesenteric lymph nodes also revealed tubular cortical sinuses that branched and

3Correspondence should be addressed to: John H. Kehrl, B-Cell Molecular Immunology Section, Laboratory of Immunoregulation, National Institute of Allergy and Infectious Disease, 10 Center Drive, MSC 1888, Bethesda, MD 20892-1752, U. S. A., Tel: 301-496-3819, Fax 301-402-0070, E-mail: jkehrl@niaid.nih.gov.

[2]C. Park and R. Sinha made equal contributions to the manuscript.

COMPETING INTEREST STATEMENT

The authors declare they have no competing financial interests.

anastomosed to other such structures (Kurokawa and Ogata, 1980). Later, labyrinth-like structures filled with lymphocytes were described in rat mesenteric lymph nodes (He, 1985). These labyrinths were found close to HEVs, underneath follicles, and likely correspond to the cortical sinus network described in the other studies. They were suggested to be involved in exit of lymphocytes from lymph nodes (He, 1985). Despite these early studies documenting cortical lymphoid sinuses, most egress studies have focused on the medullary sinus (Mandala et al., 2002).

Description of a pertussis toxin-sensitive G-protein signaling pathway needed for thymocyte emigration was the beginning of our understanding of the molecular requirement for lymphocyte egress from primary and secondary lymphoid organs (Chaffin and Perlmutter, 1991). More recently the immunosuppressive drug FTY720, its analogs, and other related molecules have shed additional light on the molecular mechanisms of lymphocyte egress (Cyster, 2005). Treatment of mice with FTY720 inhibits T cell emigration from the thymus and egress from lymph nodes (Yagi et al., 2000, Mandala et al., 2002). *In vivo* FTY720 is converted to an active phosphate moiety (FTY720-P) via the activity of the sphingolipid kinases SPHK1a and SPHK2 (Billich et al., 2003; Paugh et al., 2003). FTY720-P displays agonist activity at all of the Sphingosine 1-Phosphate (S1P) receptors with the exception of $S1P_2$ (Brinkmann et al., 2002). The absence of $S1P_1$ expression on mouse hematopoietic cells produced results reminiscent to those observed with FTY720 treatment as mature $S1P_1$ deficient T lymphocytes exited poorly from secondary lymphoid tissues and the thymus (Allende et al., 2004; Lo et al., 2005; Matloubian et al., 2004). These results argued that $S1P_1$ is an essential part of the mechanism utilized by lymphocytes for their egress from secondary lymphoid tissues and the thymus. The FTY720 results were explained by showing that FTY720-P can act as a functional antagonist triggering receptor internalization and degradation. This would make lymphocytes unresponsive to the S1P present in the efferent lymph that presumably attracts lymphocytes from the lymph node parenchyma into the medullary sinus. However, others have argued that the $S1P_1$ deficient lymphocytes are abnormal and that S1P predominantly acts on receptors present on lymphatic endothelial cells to control lymphocyte egress (Alfonso et al., 2006; Mandala et al., 2002). In this scenario FTY720-P acts as an agonist on lymphatic endothelial cells to trigger closure of the lymphatic endothelial barrier (Rosen et al., 2003). Further support for the second model has come from imaging the behavior of T cells in the medullary sinus region of the lymph node following treatment with a $S1P_1$ agonists later reversed with $S1P_1$ antagonists (Sanna et al., 2006; Wei et al., 2005).

The ultrastructural studies of lymph nodes suggest that lymphocytes not only exit by crossing the medullary sinuses, but may also enter lymphatics in the cortical region and around follicles. The presence of an exit route adjacent to the lymph node follicle makes sense as it becomes unnecessary for B cells to cross the T lymphocyte rich cortical area to enter into the medullary lymphatics. With this in mind we examined the location of lymphatics in relation to the lymph node follicle and determined whether they support the exit of B lymphocytes using conventional immunohistochemistry. Because of their relatively superficial location within the lymph node intravital two-photon laser scanning microscopy (TP-LSM) could be used to observe B cell behavior near these efferent lymphatic channels. By blocking the entrance of new cells those cells that have remained within the lymph node follicle for a defined duration could be examined in the presence or absence of S1P analogs. In addition, we have made use of B cells prepared from $S1P_3^{-/-}$ mice and from *Gnai2*$^{-/-}$ mice, which have defects in S1P mediated chemotaxis.

RESULTS

Lymphatics Adjacent to Lymph Node Follicles are Emptied of B lymphocytes by FTY720 Treatment

Thick sections of lymph node were studied with confocal microscopy after staining tissue for LYVE-1, a lymphatic endothelium-specific receptor for hyaluronan (Banerji et al., 1999), and B220 (Figure 1A). In the outer cortex of lymph nodes we observed lymphatic channels in very close proximity to follicles. These lymphatics were situated at the boundary of follicle and the T cell zone. A few follicles were seen whose complete apical surface was covered by lymphatics. Optical sectioning showed that these channels were filled with B lymphocytes. At some places these lymphatics were connected to the lymphatics in the deep cortex and medullary sinuses. A partial three dimensional reconstruction of the LYVE-1 positive structures adjacent to a lymph node follicle is shown (Figure 1B). While lymphatics around follicles were filled with B lymphocytes, lymphatics in the deep cortex mainly contained T lymphocytes and few B cells (Figure 1C).

The above results indicated that the lymphatics around the lymph node follicle support the egress of B lymphocyte from follicles. To further address this issue we gavaged mice with FTY720 to block the exit of lymphocytes into lymphatics. Confocal imaging of lymph nodes from FTY720 treated mice clearly showed that the lumen of the lymphatics around the follicles were completely devoid of B lymphocytes (Figure 1D). As the exit was blocked by FTY720, numerous B lymphocytes were found in adjacent T-area. We did not see this kind of encroachment in control lymph node sections.

Relocation of B Lymphocytes in the Lymph Node Follicle

The average residence time for B lymphocytes in lymph node is approximately 24 h. This fact and our observation that B lymphocytes leave follicle via lymphatics present along the edge of the follicle suggest that exiting B lymphocytes may move towards apical face of the follicle with time. To confirm this we adoptively transferred B lymphocytes to recipient mice and 2 hours later treated with CD62L antibody. The antibody will block further entry of lymphocytes into the lymph node (Lepault et al., 1994). Eighteen hours later we harvested lymph nodes and determined the locations of transferred B lymphocytes by immunohistochemistry. As expected the CD62L antibody treated mice had smaller follicles than did the PBS treated mice. Grossly the follicle was divided into 2 regions, the basal region that is juxtaposed to subcapsular sinus and the apical region close to cortical lymphatics (Figure 2A). In control lymph nodes in which there is a continuously replenishing of their follicular lymphocytes from peripheral blood, there were always more transferred cells in the basal compared to apical region. This suggests that after entrance into the follicle the B cells tend to localize away from the lymphatics and HEVs towards the center of the lymph node follicle. In contrast, in the antibody treated group a cohort of B lymphocytes that entered during the initial 2 hour period following transfer had moved towards apical region (Figure 2B). While on average the population of cells in the CD62L antibody treated mice moved from the basal region towards the apical region, a small population of cells remained close to the subcapsular space (Figure 2A). To better quantify the locations of the cells relative to the lymphatic regions, we measured the distances of the transferred cells in the apical region from the cortical sinusoid and those in the basal region from the subcapsular space (Figure 2C). The most striking difference was a comparison between the apical populations, while the difference between the basal populations was not statistically significant (Figure 2C).

Location of $S1P_1$+ B Lymphocytes in the Follicle

The level of $S1P_1$ receptor expression on lymphocytes is low to non-existent in peripheral blood and lymph and is up-regulated within the lymphoid tissues (Lo et al., 2005; Matloubian

et al., 2004). To study the localization of $S1P_1$+ B lymphocytes in the lymph node follicle in relation to the cortical lymphatics we performed immunohistochemistry using an $S1P_1$ specific antibody (Figure 3). The $S1P_1$ antibody was raised against amino acid residues 322–381 from human $S1P_1$, cross reacts with mouse $S1P_1$, and recognizes normal, but not $S1P_1^{-/-}$ mouse tissues (Akiyama et al., 2008). First, we verified that a control matched rabbit antibody showed no staining (Figure 3A). Next, we used the $S1P_1$ antibody and found that most follicular B cells exhibited a low intensity homogenous membrane expression (Figure 3B). We found a reduction in the membranous $S1P_1$ staining on those B cells close to the cortical lymphatics and those B cells near the subcapsular sinus as compared to the B cells deep in the follicle (magnified images from Figure 3B, supplement Figure 1S). HEVs reacted strongly with the $S1P_1$ specific antibody (Figure 3B) and the nearby LYVE-1 positive lymphatics also reacted with the antibody although the intensity of staining was less than on HEVs (Figure 3C & D). Besides the homogenous membrane expression we noted occasional punctate staining. The amount of punctate staining was higher on cells closer to the lymphatics and most of the cells within the lumen of the lymphatic exhibited this pattern suggesting that this may represent internalization of the receptor (Figure 3E). To test that possibility we examined $S1P_1$ expression on lymph node sections prepared from FTY720 treated or control mice (Figure 3F & G). B cells with punctate and cytoplasmic $S1P_1$ staining were much more numerous in the section from the FTY720 treated mice. In contrast to the B cells, we did not see punctate staining on the lymphatic and vascular endothelium although we did note a slight enhancement in the staining of the lymphatic endothelium from the FTY720 treated mice.

Imaging B Lymphocyte Egress: Long term FTY720 Treatment Decreases B Cell Motility and Blocks Egress

To determine whether the LYVE-1 antibody could be used to delineate the lymphatics near to lymph node follicles *in vivo*, we transferred fluorescently labeled splenic B cells into syngenic mice, followed 12 hours later by injection of LYVE-1 conjugated to Alexa Fluor-594 subcutaneously in the region that drains the inguinal lymph node. Twenty four hours after B cell transfer we used intravital TP-LSM to image the inguinal lymph node. We collected a 250 μm image stack (individual slices every 3μm). The LYVE-1 antibody nicely stained lymphatic structures near to the lymph node follicle similar to what we had observed using fixed samples (similar experiments using an isotype matched labeled antibody did not reveal these structures, data not shown). Transferred B cells were noted in the lumen (Figure 4A; supplement movie M1) indicating that the antibody had not blocked egress. While LYVE-1 deficient mice have normal lymphatic development and function (Gale et al., 2007) some adverse effect of the antibody on lymphocytes crossing the lymphatic endothelium remains possible. In contrast to the cortical lymphatics, many macrophages can be observed within the subcapsular sinus and medullary lymphatics (Ohtani and Ohtani, 2008). To verify that we were imaging cortical and not medullary lymphatics, we performed TP-LSM of the inguinal lymph node of a mouse previously injected with a fluorescently labeled macrophage marker CD169/sialoadhesion and with the LYVE-1 antibody. As expected the cortical lymphatics were largely devoid of CD169 positive cells (Supplementary Figure 2S). Because we wanted to image those B lymphocytes ready to exit the lymph node follicle rather than recent immigrants, we blocked further lymphocyte ingress into lymph nodes by treating the mice with CD62L antibody 18 hours prior to imaging. To verify that we had identified lymphatic structures relevant to B lymphocyte egress we compared mice treated or not with FTY720 24 hours prior to imaging. The protocol used for the imaging experiments is shown (Figure 4B). Images showing LYVE-1 staining and transferred B cells from either non-treated or FTY720 treated mice are shown (Figure 4C & D). For purposes of trafficking individual B cells we divided the lymph node into 3 regions designated c, b, and a (right panels, supplement Movies 2 & 3). In non-FTY720 treated mice the majority of the B lymphocytes resided in the lymph node follicle, some B lymphocytes resided near lymphatic region. The cells in the basal (c) region of the lymph node had a slightly

higher velocity than did those in the apical region (b) and those near the lymphatics (a) (Figure 4E). The B cells in all regions were significantly affected by FTY720 treatment with an approximately 40% reduction in their expected velocities (Figure 4F). Treatment with FTY720 moderately increased the density of B cells within the lymph node follicle presumably due to a reduction in B lymphocyte egress (Figure 4G). Tracking only those individual B cells attempting to cross the lymphatic endothelium showed that FTY720 treatment reduced their velocity and decreased their displacement as a function of the square root of time of tracking as compared to cells from non-treated mice (Figure 4H and 4I). Examination of the cells within 30 microns of a cortical lymphatic and enumeration of the percentage which engaged the endothelium for greater than 2 minutes revealed that FTY720 treatment reduced the frequency by greater than two-fold (Figure 5J).

Zoomed images of individual B cells near cortical lymphatics from a control and a FTY720 treated mouse are shown (Figure 5A and 5B). Similar to what we had observed with immunohistochemistry no transferred B cells were observed in the lumen of the lymphatics near the lymph node follicles following FTY720 treatment (Figure 5B). Imaging non-treated mice revealed that some cells approached and rapidly crossed the lymphatic endothelium, requiring approximately 2–3 minutes, while other cell meandered around the lymphatic sinusoid for several minutes prior to crossing or leaving the vicinity (Figure 5C, supplement movie M4). On rare occasions a cell crossed in the opposite direction (data not shown). Those cells that successfully crossed the endothelium appeared to do so by migrating through openings or channels in a step wise process similar to what has been described by light microscopy examining rat lymphocytes crossing the lymphatic endothelium of lacteals (Azzali, 1990). The crossing cell first engaged the endothelium, then extended a filopodial-like membrane projection into the site of passage, and finally squeezed through the channel-like opening reaching the lumen of the lymphatic vessel. Often the cell rounded up after entering into the lymphatic (Supplement Figure 3S). In contrast, we failed to observe a single B lymphocyte cross into the sinusoids in the FTY720 treated mice (Figure 5D, supplement movie M5). Some B cells hovered close to the endothelium without engaging it. Those B cells that approached the endothelium failed to penetrate it. Individual cells occasionally persisted in their attempts to cross into the sinusoid lumen however we failed to observe any cell attempting to squeeze through the endothelium as we had observed in the absence of drug. Analyzing 25 B cells in the absence of FTY720 that engaged the lymphatic endothelium for a minimum of two minutes revealed that 15 cells crossed the endothelium, 2 cells remained engaged for the duration of the imaging period without crossing, and 8 cells engaged but failed to cross. Some of the cells that crossed did so, but required several attempts before passing. In contrast among 25 cells that engaged the endothelium in FTY720 treated mice none of the cells crossed (Figure 5E).

Short Term FTY720 Treatment Blocks the Entrance of B Lymphocytes into Lymphatics, Increases Engagement with the Cortical lymphatics, but Does not Affect their Motility

To examine the short term effects of FTY720 on B lymphocyte motility and egress we performed intravital microscopy either prior to or 4 hours after FTY720 administration. In these experiments we transferred labeled B cells, 12 hours later injected the LYVE-1 antibody, and after 12 more hours prepared the mouse for imaging. After 30 min of imaging we injected FTY720 and waited 4 hours before imaging the same mouse inguinal lymph node preparation. A previous time course experiment had shown that B cells stopped crossing the LYVE-1 positive endothelium approximately two hours after administration of the drug (C. Park and J. Kehrl, unpublished observation). Shown is the same lymph node follicle before and after FTY720 (Figure 6A). In contrast to what we had observed following a 24 hour exposure to FTY720, the motility of B cells in the different regions of the lymph node follicle and close to the lymphatics remained unaffected by FTY720 treatment (Figure 6B). Tracking individual B

cells attempting to cross the lymphatic endothelium revealed no change in their average speed, but we did observe some greater variability in the displacement following FTY720 treatment (Figure 6C and 6D). In contrast to the long term FTY720 treatment where we saw a reduction in the number of cells approaching the cortical lymphatics the short term FTY720 treatment increased by approximately 50% the number of cells that engaged the endothelium. Since we imaged the same inguinal lymph node preparation before and after 4 hours after FTY720 we could observe the behavior of cells around the same cortical lymphatics. Examination of individual B cells that bound the endothelium for a minimum of two minutes revealed that 11/25 cells crossed prior to FTY720, while none of the cells after 4 hours of FTY720 crossed. Again following FTY720 treatment several cells tried to cross repeatedly without success (Figure 6F, supplement movies M6 & M7).

$S1P_3$ not $S1P_1$ mediates B Lymphocytes Chemotaxis to S1P yet $S1P_3^{-/-}$ B cells Transit through Lymph Nodes Normally

Our imaging experiments suggested as previously reported with T cells that FTY720 blocks B cells from crossing the lymphatic endothelium. Yet FTY720 treatment does not recapitulate a physiologic process and the argument that $S1P_1$ functions as a chemoattractant receptor facilitating the movement of B and T cells from the lymph node parenchyma into the efferent lymphatics remained persuasive. Therefore, we used several different approaches to test the importance of S1P-mediated chemotaxis in B lymphocyte egress. First we examined the role of $S1P_1$ in mediating B cell chemotaxis to S1P *in vitro.* To do so we examined the response of follicular B cells in standard chemotaxis assays using S1P as a chemoattractant in conjunction with a $S1P_1$ specific antagonist (VPC23019). Although at higher concentrations VPC23019 also has antagonistic activity at the $S1P_3$ receptor, we used a concentration that is relatively specific for $S1P_1$ (Davis et al., 2005). Surprisingly we found that antagonist did not diminish the S1P mediated chemotaxis response, but rather enhanced it, indicating that another S1P receptor mediates S1P directed B cell chemotaxis (Figure 7A). A previous study had shown that $S1P_3^{-/-}$ B cells responded poorly to S1P in standard chemotaxis assays (Girkontaite et al., 2004). We verified those results. $S1P_3$ deficient B cells had no detectable chemotaxis to S1P. This defect is most pronounced with marginal zone B cells, which respond better to S1P than do other B cell subsets, but follicular B cells also fail to respond (Figure 7B). We then examined whether the loss of $S1P_3$ receptors affected B cell transit through lymph nodes or the motility of B cells within the inguinal lymph node follicle or adjacent to the lymphatics. We found that the $S1P_3^{-/-}$ B behaved nearly identically to normal B cells in their entrance into lymph nodes, transit time through lymph nodes, and their motility both in the follicle and near lymphatics as assessed by adoptive transfer and TP-LSM imaging experiments (Figure 7C-E). Together these data argue that S1P triggered chemotaxis does not significantly contribute to B lymphocyte egress from lymph nodes.

Gnai2$^{-/-}$ B cells, which respond poorly to both S1P and chemokines, transit through lymph nodes more efficiently than do wild type B cells

When compared to wild type B cells, *Gnai2*$^{-/-}$ B cells home poorly to lymph nodes, respond less well in chemotaxis assays to CXCL12 and CXCL13, enter lymph node follicles poorly, and once in the follicle have a reduced interstitial velocity (Han et al., 2005). As might be predicted they also exhibit a sharp reduction in S1P mediated chemotaxis *in vitro* (Figure 8A). Yet their poor chemotatic response to chemokines and S1P does not impair their transit through lymph nodes (Figure 8B). After 18 hours of CD62L antibody treatment 60% and 74% of the transferred wild type B cells versus 74% and 92% of the transferred *Gnai2*$^{-/-}$ B cells had exited the inguinal and popliteal lymph nodes, respectively. Over the time frame examined, approximately 30% more of the *Gnai2*$^{-/-}$ B cells had exited than had wild type B cells. To facilitate the imaging of *Gnai2*$^{-/-}$ B cells we adoptively transferred twice as many cells as we did wild type cells. Intravital TP-LSM and tracking studies revealed that the *Gnai2*$^{-/-}$ B cells

moved slower, with less displacement, and less straight than did the wild type cells both in the middle of the follicle and near the LYVE-1 defined cortical lymphatics (Figure 8C). Nearly twice as many wild type cells localized to the center of the follicle as did the *Gnai2*$^{-/-}$ B cells while the ratio was nearly reversed near the lymphatics (Supplementary Figure 3S). The location of *Gnai2*$^{-/-}$ B cells versus wild type B cells along with cell tracks over a 30 minute imaging period are shown (Figure 8D). During 1.5 hours of imaging we observed more *Gnai2*$^{-/-}$ B cells crossing into the lymphatics adjacent to the lymph node follicle than we did wild type B cells (Figure 8E). Measuring the distances from the edge of LYVE-1 defined lymphatics in surrounding 200 × 200 × 20 μm^3 spaces of 100 control and 100 *Gnai2*$^{-/-}$ B cells also demonstrated the more proximal localization of *Gnai2*$^{-/-}$ B cells compared to control cells. Very similar results were found with pertussis toxin treated B cells as compared to non treated B cells (Supplementary Figure 4S).

DISCUSSION

The above findings aid our understanding of B lymphocyte trafficking through lymph nodes, provide insights into the role of S1P in the regulation of B lymphocyte egress from lymph nodes, and delineate the major effect of FTY720 on B lymphocyte retention in lymph nodes. The ready access of B lymphocytes to cortical lymphatic sinusoids provides an elegant solution for B lymphocyte lymph node egress. The re-localization of B cells that have resided in the lymph node longer towards the cortical lymphatics is consistent with that being a major site of egress. We also noted a population of B cells that resided close to the subcapsular sinus and an occasional transferred B cell within the sinus suggesting that it may also be a site of B cell egress however, we never observed a cell crossing from the lymph node follicle into the sinus. The levels of $S1P_1$ expression correlated with the known sources of S1P within the lymph node, as those B cells close to the subcapsular space and those cells close to the cortical lymphatic sinusoids had lower levels of $S1P_1$ expression. In addition, cells within the lymphatics had a punctate staining pattern, likely evidence of receptor internalization (Watterson et al., 2002). FTY720 treatment of mice also caused a punctate staining pattern on the majority of B cells in the lymph node follicle. Intravital TP-LSM allowed the imaging of cells around the cortical lymphatic sinusoids and the visualization of cells as they squeezed through the lymphatic endothelium. The B lymphocytes near to the lymphatics tended to move slower than did those in the center of the follicle. Treatment with FTY720 resulted in an inability of B lymphocytes to enter into the cortical lymphatic sinusoids a result similar to that described with T cells near medullary lymphatics. While short-term exposure to FTY720 did not impact the motility of B cells in the follicle, 24 hours after injection of FTY720 many B cells had slowed. Finally the *in vitro* studies of S1P chemotaxis and the *in vivo* experiments with $S1P_3^{-/-}$ B cells and *Gnai2*$^{-/-}$ B cells argue that S1P mediated chemotaxis as measured in *in vitro* chemotaxis assays is of minor importance for B lymphocyte egress. These results are compared and contrasted to previous multiphoton imaging studies of mouse T lymphocytes in mice treated with various S1P analogues or pertussis toxin in the discussion below.

As detailed in the introduction previous light microscopic studies of rodent lymph nodes, colloidal carbon injection into afferent lymphatics of rat inguinal nodes, scanning electron microscopy of injection casts from rabbit mesenteric lymph nodes, and the identification of labyrinth-like structures extending beneath follicles all provided evidence for the existence of cortical sinusoids that could provide egress sites for B lymphocytes (Anderson and Anderson, 1975; Kurokawa and Ogata, 1980; Soderstrom and Stenstrom, 1969; He, 1985). Yet their significance has not been fully appreciated as B cells are commonly thought to exit in the lymph node medulla by crossing into the medullary sinus. In the course of our studies a published report identified LYVE-1 positive lymphatic sinusoids in the neighborhood of lymph node follicles; however, the focus of that study was the role of CCR7 and $S1P_1$ receptors in the egress of T lymphocytes from lymph nodes (Pham et al., 2008). In this study we used thick

sections of the inguinal lymph nodes stained for B220 and LYVE-1, which gave a greater appreciation of the extent of the cortical sinusoids. The cortical sinusoids near to lymph node follicles were predominately filled with B lymphocytes while T cells filled the deep cortical lymphatic sinusoids. As expected, treating mice with FTY720 emptied the cortical sinusoids of lymphocytes providing additional evidence that these structures provide a major site of egress for B lymphocytes. While we have focused on the role of cortical lymphatics in mediating B lymphocyte egress for those lymph node follicles located close to the medulla, the medullary lymphatics may serve as egress sites for them.

The precise mechanism by which $S1P_1$ regulates lymphocyte egress from lymphoid organs has been surprisingly difficult to delineate. Two major models have been proposed although a hybrid model is likely to emerge to resolve the differences (Cahalan and Parker, 2008). Much of the controversy initially revolved around reconciling data from the analysis of mice reconstituted with fetal liver from $S1P_1$ deficient mice and mice treated with FTY720. One model argued for the importance of lymphocyte expressed $S1P_1$. Compelling data supports a role for the $S1P_1$ receptor as a chemoattractant receptor (Cyster, 2005). The presence of S1P lyases in the tissues creates a S1P gradient between the lymph node parenchyma and the lymph. Disruption of that gradient impairs lymphocyte egress (Schwab et al., 2005). Like other chemoattractant receptors the $S1P_1$ couples to the heterotrimeric G-protein G_i (Okamoto et al., 1998). B and T cells express significant levels of the $S1P_1$ receptor and a S1P gradient *in vitro* causes T and B lymphocytes to migrate, albeit a relatively small percentage of them do so (Allende et al., 2004; Lo et al., 2005; Matloubian et al., 2004). Like other chemoattractant receptors, S1P-triggered chemotaxis is blocked by pertussis toxin, which modifies $G_{i\alpha}$ such that receptors no longer trigger $G_{i\alpha}$ nucleotide exchange. However, other data complicates this picture. The administration of $S1P_1$ antagonists to mice has not recapitulated the phenotype observed with FTY720 (Sanna et al., 2006). Lymphocytes also express several S1P receptors in addition to $S1P_1$. $S1P_3$, not $S1P_1$, mediates marginal zone B cell chemotaxis, yet $S1P_1$ is functionally important to properly localize cells in the marginal zone while $S1P_3$ is not (Cinamon et al., 2004; Girkontaite et al., 2004). Here we also show that follicular B cells also use $S1P_3$, not $S1P_1$, to trigger S1P-mediated chemotaxis. $S1P_3^{-/-}$ B cells did not respond in a S1P chemotaxis assay and a $S1P_1$ antagonist did not inhibit S1P mediated chemotaxis. Yet $S1P_3$ deficient B cells transited through lymph nodes relatively normally. While these results argue that the $S1P_1$ receptor does not mediate B lymphocyte chemotaxis, there remains a possibility that $S1P_1$ functions *in vivo* as a chemoattractant receptor via a mechanism not modeled by current *in vitro* assays.

That the $S1P_1$ receptors, and presumably $S1P_3$ receptors, on lymph node B cells have been engaged is supported by the immunohistochemistry data, which demonstrated evidence of $S1P_1$ receptor downregulation and internalization particularly around and within the cortical lymphatic sinusoids. The enrichment of exiting B cells around the cortical lymphatics and the altered frequencies at which B cells approached the lymphatic endothelium following FTY720 treatment suggests that one consequence of S1P signaling is to retain B cells, which have meandered away from the follicle center, near the cortical lymphatics. Since $S1P_1$ receptor agonism inhibits the entry of tissue T cells into afferent lymphatics by arresting T cells at the basal surface of lymphatic vessels (Ledgerwood et al., 2008), one possibility is that $S1P_1$ receptor signaling enhances B cell adhesion to stromal elements and/or the lymphatic endothelium. Our imaging data provides some support for an S1P mediated increase in B cell adhesion to the lymphatic endothelium. Short term FTY720 treatment, which may have agonistic effects on B cell S1P receptors, caused a relative increase in the cells adjacent to the lymphatic endothelium, while 24 hours of FTY720 treatment, which should have reduced S1P receptor expression, decreased the number of cells contacting the endothelium. However, arguing against this possibility no essential role for α_4 and β_2 integrins was found for T lymphocyte lymph node egress (Lo et al., 2005). Alternatively, since intranodal chemokines

provide retention signals for T cell (Hwang et al., 2007; Pham et al., 2008) and B cells (this study), $S1P_1$ receptor signaling could directly interfere with those and thereby bias the cells towards egress. It has been reported that S1P can interfere with responses to chemokines (Graeler et al., 2002) and it is well known that signaling through one G-protein coupled receptor (GPCR) can decrease signaling through another. Mechanisms include the activation of G-protein receptor kinases (GRK); the down modulation of Gα subunits; and increased expression of Regulators of G-protein Signaling (RGS) (Reiter and Lefkowitz, 2006; Kehrl, 2006). Finally, a third possibility is that it is $S1P_3$ receptors that help promote the localization of B cells around the cortical lymphatics, however, in their absence no significant impact on trafficking through the lymph node occurs.

The other major model, which argues that $S1P_1$ receptors on endothelial cells are the major regulator of lymphocyte egress, also has considerable support (Rosen et al., 2003). In this model endothelial $S1P_1$ agonism shuts the endothelial portals. Imaging studies of explanted lymph nodes and intravital microscopy have provided major support for this model (Sanna et al., 2006; Wei et al., 2005). Two previous studies have imaged T cells intravitally using fluorescently labeled wheat germ agglutinin to label the lymphatic vessels, however, in only one of those studies were individual cells visualized crossing the medullary lymphatic endothelium (Nombela-Arrieta et al., 2007; Sanna et al., 2006). The most comprehensive study of T lymphocytes crossing into the medullary sinus was performed using explanted lymph nodes, which offers certain advantages, but disrupts the blood supply and normal flow of lymph (Wei et al., 2005). In that study T cells moved slower in the medullary region than they did in the lymph node cortex. That result has been verified by intravital microscopy (Nombela-Arrieta et al., 2007; Sanna et al., 2006). The exposure of explanted lymph nodes to the $S1P_1$ agonist SEW2871 caused T lymphocytes in the medullary region to slow further without affecting the basal velocity of the cells in the cortical region of the lymph node (Wei et al., 2005). The SEW2871-mediated medullary T lymphocyte slowing could be reversed by the addition of a competitive $S1P_1$ antagonist. In contrast, we did not observe any effect of short term effect of FTY720 exposure on the average motility of B cells either in the follicle or near the cortical lymphatics. While the results are not directly comparable, we also imaged the inguinal lymph node following treatment of mice with SEW2871 without any observed effect on the velocity of B cells (C. Park, unpublished observation). One possible explanation for this difference is that inhibiting lymphocyte egress with $S1P_1$ agonists causes more “log jamming” in the medullary region than it does around the cortical lymphatics. Alternatively, differences between B and T lymphocytes in their S1P response profiles may exist. Imaging of T lymphocytes in the T cell zone of explanted lymph nodes 24 hours after FTY720 exposure revealed no change in the velocity of the cells (Huang et al., 2007), while we observed a slowing of follicular B cells after a similar duration of drug treatment. Imaging the SEW2871 treated lymph nodes also revealed an inability of T lymphocytes to enter the medullary sinus that was reversible by adding a $S1P_1$ antagonist (Wei et al., 2005). Similarly within 2 hours of the administration of FTY720 to mice no B lymphocyte could be observed to enter into the cortical lymphatic sinusoids. The behavior of the B lymphocytes attempting to cross the lymphatic endothelium recapitulated the description of T lymphocyte behavior attempting to cross the medullary lymphatic endothelium. Some B lymphocytes pushed repeatedly against the lymphatic endothelium without breaching it, a result consistent with the possibility that the lymphatic endothelium portals are closed. Alternatively, an $S1P_1$ lymphocyte signal is needed for the B cells to negotiate its way through the endothelium.

Overall our data underscores the importance of cortical lymphatic sinusoids for B lymphocyte egress. The major effect of FTY720 treatment is to prevent B cells from crossing the endothelium, not engaging it. No requirement for S1P-triggered chemotaxis in B lymphocyte egress from the lymph node into the efferent lymphatics was found. The reduction of B cell motility following a 24 hour FTY720 exposure suggests that either S1P receptor antagonism

blocks S1P receptor-mediated signaling that augments B cell motility or, conversely, that prolonged S1P receptor agonism reduces chemokine responsiveness. Ours and others studies lead us to the following model of B lymphocyte lymph node transit. B cells enter the lymph node cortical ridge through HEVs and within 1–2 hours enter into the follicle moving towards the follicle center and reacquiring their $S1P_1$ and $S1P_3$ receptors. In the absence of antigen activation, over the next 12–18 hours the cells gradually lose responsiveness to CXCL13 freeing the cells to move back towards the follicle edge and cortical lymphatics where they are likely to sense S1P. Several different mechanisms may account for a reduction in CXCL13 responsiveness including CXCR5 desensitization. The journey to the center of the lymph node follicle can be short circuited by inhibiting chemokine receptor signaling. This allows cells to remain near the cortical lymphatics potentially facilitating their egress. Although the $S1P_3^{-/-}$ B cells exited lymph nodes similar to wild type cells, a reasonable role for the $S1P_3$ receptor would be to help localize cells towards the cortical lymphatics. Once in the neighborhood of the cortical lymphatics B cells will periodically encounter the lymphatic endothelium. Here a lymphocyte $S1P_1$ signal is needed to facilitate the cell's passage through the lymphatic endothelium. Why $S1P_3$, which can mediate S1P chemotaxis, cannot provide this signal remains enigmatic. The ability to image B and T cells crossing the cortical lymphatic sinusoids to enter into the efferent lymph should provide a valuable tool for future studies of lymphocyte trafficking through lymph nodes and across endothelial surfaces.

EXPERIMENTAL PROCEDURES

Mice

Wild-type C57BL/6J (CD45.2) and congenic strain B6.SJL (CD45.1) mice of age between 8–14 wk were purchased from Taconic. *Gnai2*$^{-/-}$ mice were originally developed by Dr. Lutz Birnbaumer (NIEHS, NIH). The $S1P_3^{-/-}$ mice were kindly provided by Dr. Richard L. Proia (NIAMSD, NIH) They were housed under specific pathogen-free conditions and used in accordance with the guidelines from the Institutional Animal Care Committee at the National Institutes of Health.

Reagents

The following anti-mouse antibodies were used: B220-Alexa Fluor-488, CD3-Alexa Fluor-647, CD8-biotin, CD4-biotin, CD11c-biotin, Gr-1-biotin, CD45.2-biotin, CD62L (BD Biosciences), CD169 (AbD Serotec), LYVE-1 (R&D Systems), $S1P_1$ (Cat # sc-25489, Santa Cruz), CD21-FITC, CD23-PE-Cy7, IgD-PE, IgM-APC (E-Biosciences). Anti-goat IgG-Alexa Fluor-633 (Invitrogen), anti-goat IgG-Rhodamine Red-X, anti-rabbit IgG-Rhodamine Red-X, streptavidin-Rhodamine Red-X and normal donkey serum (Jackson ImmunoResearch) were also used. Dynabeads M-280 streptavidin was purchased from Dynal Biotech. FTY720 was kindly provided by Volker Brinkmann (Novartis Pharmaceutical). D-erythro-sphingosine 1-phosphate and VPC23019 were purchased from Avanti Polar Lipids. RPMI 1640 medium supplemented with 2 mM L-glutamine and 25mM HEPES, charcoal-dextran filtered FBS, penicillin/streptomycin solution (10,000 IU/ml each) and 100 mM sodium pyruvate were purchased from Hyclone. Murine CCL19 and CXCL12 were purchased from R&D Systems. Fatty acid free bovine serum albumin (FAF-BSA) was purchased from Sigma-Aldrich.

Adoptive B Lymphocyte Transfer for Immunohistochemistry

The donor (CD45.2+) splenic B lymphocytes were isolated by negative depletion using biotinylated antibodies to CD4, CD8, CDllc and GR-1, and Dynabeads M-280 streptavidin. The cell purity was approximately 95%. 20 million B lymphocytes were injected into the tail vein of recipient (CD45.1+). Two hours later one group of mice (n=3) received 100 μg of CD62L antibody in the tail vein and the other group (n=3) received PBS to serve as a control.

After 17–18 hours of antibody injection all mice were killed and lymph nodes and spleens were harvested for immunohistochemistry and flow cytometry.

FTY720 Treatment

For the immunocytochemistry mice were gavaged either 1 mg/kg body weight FTY720 or PBS as a control (n=3mice/group). After 18 hours mice were killed and lymph nodes and spleen were harvested. A few lymph nodes were fixed in 4% paraformaldehyde for thick section confocal imaging. Other lymph nodes and spleen were used in flow cytometry to enumerate number of B lymphocytes in FTY720 treated versus untreated group. For the intravital microscopy experiments see below.

Immunostaining

For making thick 100 μm lymph node sections, freshly isolated nodes were fixed in a 4% paraformaldehyde solution in PBS over night at 4°C. Fixed lymph nodes were individually placed in a 24 well-plate and poured melted (37–38°C) 1.5% agarose in PBS over them. Solidified blocks of agarose containing lymph node were glued on a tissue holder in a Leica VT1000 S Vibratome and 100 μm slices were cut in a bath of ice-cold PBS. The sections were stained with the indicated antibodies. Briefly, sections were placed in an individual well of a 24 well-plate in 0.2% Triton X-100 in PBS at room temp. After incubation for 2–3 hours the detergent solution was drained and sections were submerged in 10% blocking serum for 2–3 hours at room temp. The sections were then put in 10% blocking serum containing primary antibodies (1–2 μg) over night at 4°C. Next day sections were washed for at least 2 hours at room temp with several changes of PBS. The sections were then treated with fluorescent tagged secondary antibodies and washed as it was done with primary antibodies. The tissue sections were slowly rocked during all the incubations. Finally, the section were put on a glass slide and mounted in anti-fade medium (Invitrogen). Microscopy was performed with a Leica TCS SP5 confocal microscope and images were processed in Adobe Photoshop CS and Imaris v. 6.0.1 (Bitplane). In some experiments freshly isolated lymph nodes were snap frozen in Tissue-Tek OCT compound (Sakura Finetek). Six μm frozen sections were stained using a standard technique. Images were acquired with a Leica TCS SP5 confocal microscope.

Intravital Two-Photon Microscopy and Analysis

Inguinal lymph nodes were prepared for intravital microscopy using a slightly modification of a previously described method (Han et al., 2005). Splenic B cells prepared from C57BL/6 mice were labeled for 15 min at 37 °C with 5 μM CMFDA or 50 μm CMF_2HC. Ten million labeled cells in 200 μl of PBS were adoptively transferred by tail vein injection into 6~10-week-old recipient mice. For long term exposure to FTY720 mice were injected with FTY720 (1.5 mg/kg body weight) or vehicle by intraperitoneal injection 24 hours after cell transfer. Six hours later recipient mice were injected intravenously with CD62L antibody (100 μg per mouse) to block further lymphocytes ingress into the lymph node. Twelve hours prior to imaging mice were injected subcutaneously with 20 μg of LYVE-1 antibody conjugated with Alexa Fluor-594 in 200 μl PBS close to the inguinal lymph node. After anaesthetizing the mice by intraperitoneal injection 300 mg/kg of Avertin (tribromoethanol, Sigma), the skin and fatty tissue over inguinal lymph node were removed. To visualize both the B cell follicle and the lymphatic area in the same imaging field, the exposed inguinal lymph node was gently rotated 90° from its original orientation. The mouse was placed in a pre-warmed coverglass chamber slide (Nalgene, Nunc). The chamber slide was then placed into the temperature control chamber (The Cube and Box, Life Imaging Services) equipped on the Leica SP5 microscope. The temperature of air was monitored and maintained at 37.0 °C± 0.5 °C. Inguinal lymph node was intravitally image from the capsule over a range of depths (60–220 μm). For short term exposure to FTY720 recipient mice were prepared similar to the above procedure. The recipient mice

were injected with FTY720 following initial imaging and then 4 hours later the same field imaged again. The CD62L antibody was not used in the short term FTY720 experiments. Two-photon imaging was performed with a Leica SP5 inverted 5 channel confocal microscope (Leica Microsystems) equipped with 20x multi-immersion objective, 0.7 NA (immersion medium used was 80% glycerol). Two-photon excitation was provided by a Mai Tai Ti:Sapphire laser (Spectra Physics) with a 10 W pump, tuned to 810 nm. For four-dimensional analysis of cell migration, stacks of 4 or 10 section (z step = 3 μm) were acquired every 15 or 30 sec to provide an imaging volume of 9 or 27 μm in depth. Emitted fluorescence was collected using a 4 channel non-descanned detector. Wavelength separation was through a dichroic mirror at 495 nm and then separated again through a dichroic mirror at 455 nm followed by 405/20 nm emission filter for second harmonics and 480/40 nm emission filter for CMF_2HC; a dichroic mirror at 565 nm followed by 525/50 nm emission filter for CMFDA and 620/60 nm emission filter for AlexaFluor-594. Sequences of image stacks were transformed into volume-rendered four-dimensional movies using Imaris software and spot analysis was used for semi-automated tracking of cell motility in three dimensions by using the following parameters: autoregressive motion algorithm, estimated diameter 10 μm, background subtraction true, maximum distance 20 μm, and maximum gap size 3. The data set was corrected for tissue drift and calculations of the cell velocity and displacement were performed using the Imaris software. All statistical analysis was performed with GraphPad Prism (GraphPad Software). Significance of statistics was calculated with unpaired t test for two nonparametric data and with Kruskal-Wallis test for three nonparametric data.

Chemotaxis

Chemotaxis assays were performed using a transwell chamber (Costar) as previously described (Moratz et al. 2004). Cells were added in a volume of 100 μl to the upper wells of a 24-well Transwell plate with a 5-μm insert. Lower wells contained 600 μl of assay medium with various concentrations of chemokines and lipids. The number of cells that migrated to the lower well following a three hour incubation at 37°C were counted using a flow cytometer. The percent migration was determined by first taking the difference between the number of transmigrating cells of a given subset in the presence of chemoattractant from those where no chemoattractant was present. The fraction of migrated cells obtained for each condition was divided by the total number of cells of that subset in the starting cell suspension. The results were multiplied by 100 and graphs of the data were generated (Prism; Graphpad Software).

Homing and Lymph node transit assays

B cells from control and experimental mice were labeled with 1 μM CMFDA or 2.5 μM CMTMR for 15 min at 37 °C and seven to twenty million cells of each population were injected intravenously to recipient mice. After 2 hr, spleen, inguinal lymph nodes, and popliteal lymph nodes were removed, and gently dissociated into single cell suspensions. Peripheral blood was collected by retro-orbital eye bleeding. After removing red blood cells with Tris-NH_4Cl, the cells were resuspended in PBS containing 1% BSA at 4 °C. Flow cytometric analysis was performed on a BD FACS Calibur flow cytometer and the data were analyzed using the FlowJo software (Tree Star, Inc., San Carlos, CA). Forward and side scatter parameters were used to gate on live cells. The lymph node transit assay used a similar initial approach, but two hours after the cell transfer the control and experimental mice were injected intravenously with CD62L antibody (100 μg/mouse) for each time point. After indicated duration the spleen, lymph nodes, and peripheral blood were collected and cell numbers determined as in the homing assay. The ratios between the numbers of cells in the various compartments two hours after transfer versus after CD62L antibody injection were calculated.

Supplementary Material

Refer to Web version on PubMed Central for supplementary material.

Acknowledgments

The authors would like thank Mary Rust for her editorial assistance; Dr. Anthony Fauci for his continued support; and Dr. Owen Schwartz, Meggan Czapiga, and Dr. Juraj Kabat of the Research Technology Branch of the National Institutes of Allergy and Infectious Diseases for their help in the acquisition and analysis of the TP-LSM data. This research was supported by the Intramural Research Program of the National Institute of Allergy and Infectious Diseases, National Institutes of Health.

References

Akiyama T, Sahahira Y, Matsubara K, Mori M, Igarashi Y. Immunohistochemical detection of sphingosine-1-phosphate receptor 1 in vaxcular and lymphatic endothelial cells. J Mol Histol 2008;39:527–533. [PubMed: 18758970]

Alfonso C, McHeyzer-Williams MG, Rosen H. CD69 down-modulation and inhibition of thymic egress by short- and long-term selective chemical agonism of sphingosine 1-phosphate receptors. Eur J Immunol 2006;36:149–159. [PubMed: 16342326]

Allende ML, Dreier JL, Mandala S, Proia RL. Expression of the sphingosine 1-phosphate receptor, S1P1, on T-cells controls thymic emigration. J Biol Chem 2004;279:15396–15401. [PubMed: 14732704]

Anderson AO, Anderson ND. Studies on the structure and permeability of the microvasculature in normal rat lymph nodes. Am J Pathol 1975;80:387–418. [PubMed: 1163637]

Azzali G. The passage of macrophages and lymhocytes from the interstitium across the lymphatic endothelium of rat lacteals. Cell and Tissue Res 1990;262:191–193. [PubMed: 2257610]

Banerji S, Ni J, Wang SX, Clasper S, Su J, Tammi R, Jones M, Jackson DG. LYVE-1, a new homologue of the CD44 glycoprotein, is a lymph-specific receptor for hyaluronan. J Cell Biol 1999;144:789–801. [PubMed: 10037799]

Billich A, Bornancin F, Devay P, Mechtcheriakova D, Urtz N, Baumruker T. Phosphorylation of the immunomodulatory drug FTY720 by sphingosine kinases. J Biol Chem 2003;278:47408–47415. [PubMed: 13129923]

Brinkmann V, Davis MD, Heise CE, Albert R, Cottens S, Hof R, Bruns C, Prieschl E, Baumruker T, Hiestand P, et al. The immune modulator FTY720 targets sphingosine 1-phosphate receptors. J Biol Chem 2002;277:21453–21457. [PubMed: 11967257]

Cahalan MD, Parker I. Choreography of Cell Motility and Interaction Dynamics Imaged by Two-Photon Microscopy in Lymphoid Organs. Annu Rev Immunol 2008;26:585–626. [PubMed: 18173372]

Chaffin KE, Perlmutter RM. A pertussis toxin-sensitive process controls thymocyte emigration. Eur J Immunol 1991;21:2565–2573. [PubMed: 1655469]

Cinamon G, Matloubian M, Lesneski MJ, Xu Y, Low C, Lu T, Proia RL, Cyster JG. Sphingosine 1-phosphate receptor 1 promotes B cell localization in the splenic marginal zone. Nat Immunol 2004;5:713–720. [PubMed: 15184895]

Cyster JG. Chemokines, sphingosine-1-phosphate, and cell migration in secondary lymphoid organs. Annu Rev Immunol 2005;23:127–159. [PubMed: 15771568]

Davis MD, Clemens JJ, Macdonald TL, Lynch KR. Sphingosine 1-phosphate analogs as receptor antagonists. J Biol Chem 2005;280:9833–9841. [PubMed: 15590668]

Gale NW, Prevo R, Espinosa J, Ferguson DJ, Yancopoulos GD, Thurston G, Jackson DG. Normal lymphatic development in mice deficient for the lymphatic hyaluronan receptor LYVE-1. Mol Cell Biol 2007;27:595–604. [PubMed: 17101772]

Girkontaite I, Sakk V, Wagner M, Borggrefe T, Tedford K, Chun J, Fischer KD. The sphingosine-1-phosphate (S1P) lysophospholipid receptor S1P3 regulates MAdCAM-1+ endothelial cells in splenic marginal sinus organization. J Exp Med 2004;200:1491–1501. [PubMed: 15583019]

Gowans JL. The effect of the continuous re-infusion of lymph and lymphocytes on the output of lymphocytes from the thoracic duct of unanaesthetized rats. Br J Exp Pathol 1957;38:67–78. [PubMed: 13413083]

Graeler M, Shankar G, Goetzl EJ. Cutting edge: suppression of T cell chemotaxis by sphingosine 1-phosphate. J Immunol 2002;169:4084–4087. [PubMed: 12370333]

Hall JG, Morris B. The Origin of the Cells in the Efferent Lymph from a Single Lymph Node. J Exp Med 1965;121:901–910. [PubMed: 14319406]

Han SB, Moratz C, Huang NN, Kelsall B, Cho H, Shi CS, Schwartz O, Kehrl JH. Rgs1 and Gnai2 regulate the entrance of B lymphocytes into lymph nodes and B cell motility within lymph node follicles. Immunity 2005;22:343–354. [PubMed: 15780991]

He Y. Scanning electron microscope studies of the rat mesenteric lymph node with special reference to high-endothelial venules and hitherto unknown lymphatic labyrinth. Arch Histol Jpn 1985;48:1–15. [PubMed: 4015330]

Huang JH, Cardenas-Navia LI, Caldwell CC, Plumb TJ, Radu CG, Rocha PN, Wilder T, Bromberg JS, Cronstein BN, Sitkovsky M, et al. Requirements for T lymphocyte migration in explanted lymph nodes. J Immunol 2007;178:7747–7755. [PubMed: 17548612]

Kehrl JH. Chemoattractant receptor signaling and the control of lymphocyte migration. Immunol Res 2006;34:211–227. [PubMed: 16891672]

Kurokawa T, Ogata T. A scanning electron microscopic study on the lymphatic microcirculation of the rabbit mesenteric lymph node. A corrosion cast study. Acta Anat (Basel) 1980;107:439–466. [PubMed: 6996414]

Ledgerwood LG, Lal G, Zhang N, Garin A, Esses SJ, Ginhoux F, Merad M, Peche H, Lira SA, Ding Y, et al. The sphingosine 1-phosphate receptor 1 causes tissue retention by inhibiting the entry of peripheral tissue T lymphocytes into afferent lymphatics. Nat Immunol 2008;9:42–53. [PubMed: 18037890]

Lepault F, Gagnerault MC, Faveeuw C, Boitard C. Recirculation, phenotype and functions of lymphocytes in mice treated with monoclonal antibody MEL-14. Eur J Immunol 1994;24:3106–3112. [PubMed: 7528669]

Lo CG, Xu Y, Proia RL, Cyster JG. Cyclical modulation of sphingosine-1-phosphate receptor 1 surface expression during lymphocyte recirculation and relationship to lymphoid organ transit. J Exp Med 2005;201:291–301. [PubMed: 15657295]

Mandala S, Hajdu R, Bergstrom J, Quackenbush E, Xie J, Milligan J, Thornton R, Shei GJ, Card D, Keohane C, et al. Alteration of lymphocyte trafficking by sphingosine-1-phosphate receptor agonists. Science 2002;296:346–349. [PubMed: 11923495]

Matloubian M, Lo CG, Cinamon G, Lesneski MJ, Xu Y, Brinkmann V, Allende ML, Proia RL, Cyster JG. Lymphocyte egress from thymus and peripheral lymphoid organs is dependent on S1P receptor 1. Nature 2004;427:355–360. [PubMed: 14737169]

Nombela-Arrieta C, Mempel TR, Soriano SF, Mazo I, Wymann MP, Hirsch E, Martinez AC, Fukui Y, von Andrian UH, Stein JV. A central role for DOCK2 during interstitial lymphocyte motility and sphingosine-1-phosphate-mediated egress. J Exp Med 2007;204:497–510. [PubMed: 17325199]

Okamoto H, Takuwa N, Gonda K, Okazaki H, Chang K, Yatomi Y, Shigematsu H, Takuwa Y. EDG1 is a functional sphingosine-1-phosphate receptor that is linked via a Gi/o to multiple signaling pathways, including phospholipase C activation, Ca2+ mobilization, Ras-mitogen-activated protein kinase activation, and adenylate cyclase inhibition. J Biol Chem 1998;273:27104–27110. [PubMed: 9765227]

Ohtani O, Ohtani Y. Structure and function of rat lymph nodes. Arch Histol Cytol 2008;71:69–76. [PubMed: 18974599]

Paugh SW, Payne SG, Barbour SE, Milstien S, Spiegel S. The immunosuppressant FTY720 is phosphorylated by sphingosine kinase type 2. FEBS Lett 2003;554:189–193. [PubMed: 14596938]

Pham TH, Okada T, Matloubian M, Lo CG, Cyster JG. S1P1 receptor signaling overrides retention mediated by G alpha i-coupled receptors to promote T cell egress. Immunity 2008;28:122–133. [PubMed: 18164221]

Reiter E, Lefkowitz RJ. GRKs and beta-arrestins: roles in receptoro silencing, trafficking, and signaling. Trends Endocrin Metab 2006;17:159–165.

Rosen H, Sanna G, Alfonso C. Egress: a receptor-regulated step in lymphocyte trafficking. Immunol Rev 2003;195:160–177. [PubMed: 12969317]

Sanna MG, Wang SK, Gonzalez-Cabrera PJ, Don A, Marsolais D, Matheu MP, Wei SH, Parker I, Jo E, Cheng WC, et al. Enhancement of capillary leakage and restoration of lymphocyte egress by a chiral S1P1 antagonist in vivo. Nat Chem Biol 2006;2:434–441. [PubMed: 16829954]

Schwab SR, Pereira JP, Matloubian M, Xu Y, Huang Y, Cyster JG. Lymphocyte sequestration through S1P lyase inhibition and disruption of S1P gradients. Science 2005;309:1735–1739. [PubMed: 16151014]

Soderstrom N, Stenstrom A. Outflow paths of cells from the lymph node parenchyma to the efferent lymphatics--observations in thin section histology. Scand J Haematol 1969;6:186–196. [PubMed: 4896308]

Watterson KR, Johnston E, Chalmers C, Pronin A, Cook SJ, Benovic JL, Palmer TM. Dual regulation of EDG1/S1P(1) receptor phosphorylation and internalization by protein kinase C and G-protein-coupled receptor kinase 2. J Biol Chem 2002;277:5767–5777. [PubMed: 11741892]

Wei SH, Rosen H, Matheu MP, Sanna MG, Wang SK, Jo E, Wong CH, Parker I, Cahalan MD. Sphingosine 1-phosphate type 1 receptor agonism inhibits transendothelial migration of medullary T cells to lymphatic sinuses. Nat Immunol 2005;6:1228–1235. [PubMed: 16273098]

Yagi H, Kamba R, Chiba K, Soga H, Yaguchi K, Nakamura M, Itoh T. Immunosuppressant FTY720 inhibits thymocyte emigration. Eur J Immunol 2000;30:1435–1444. [PubMed: 10820391]

Young AJ. The physiology of lymphocyte migration through the single lymph node in vivo. Semin Immunol 1999;11:73–83. [PubMed: 10329494]

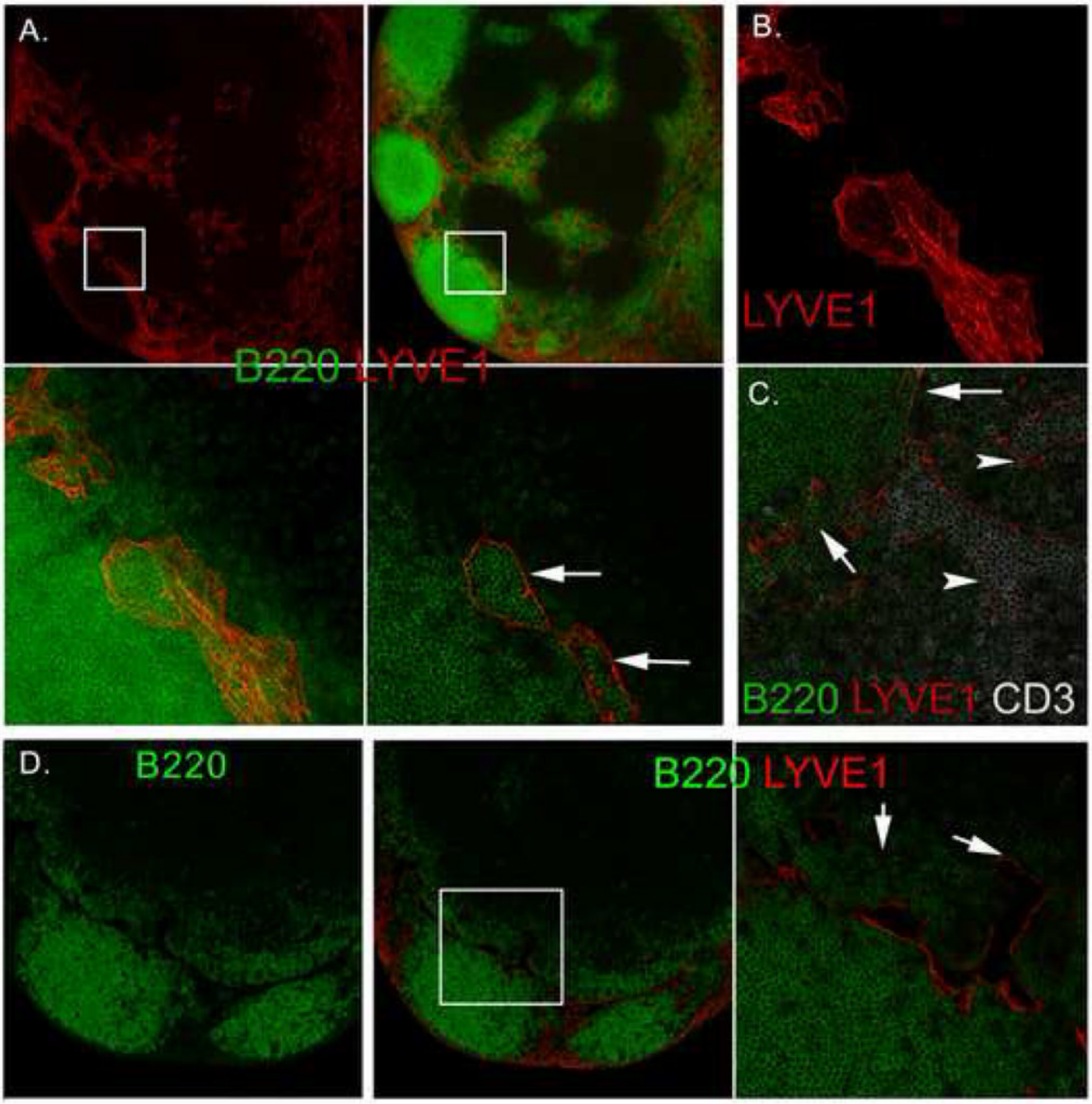

Figure 1.

LYVE-1 positive lymphatics adjacent to the lymph node follicles are emptied by FTY720 treatment. (A) Confocal images of untreated lymph node sections immunostained for LYVE-1 and B220. The top left panel shows LYVE-1 staining alone and top right panel B220 and LYVE-1 using a 100 μm thick section. The bottom left panel shows a 5X zoomed image of the B220 and LYVE-1 stained section (white square). The bottom right image shows a single optical section. Arrows show B cells within LYVE-1 positive lymphatic. (B) 100 μm lymph node section immunostained with for LYVE-1 and optically sectioned by confocal microscopy. (C) A section from the lymph node follicle and T cell zone interface immunostained for B220, LYVE-1, and CD3. T cell zone lymphatics indicated with an arrow-head and those adjacent

to the lymph node follicle indicated with an arrow. (D) Lymph node from FTY720 treated mice and immunostained for B220 and LYVE-1. Left and middle panels show B220, and B220 and LYVE-1 staining, respectively. Right panel is a 4X zoomed image of the lymph node follicle/T cell zone interface (white square in previous image) immunostained with B220 and LYVE-1. Empty lymphoid sinuses in the B cell zone (left arrow) and T cell zone (right arrow) are indicated.

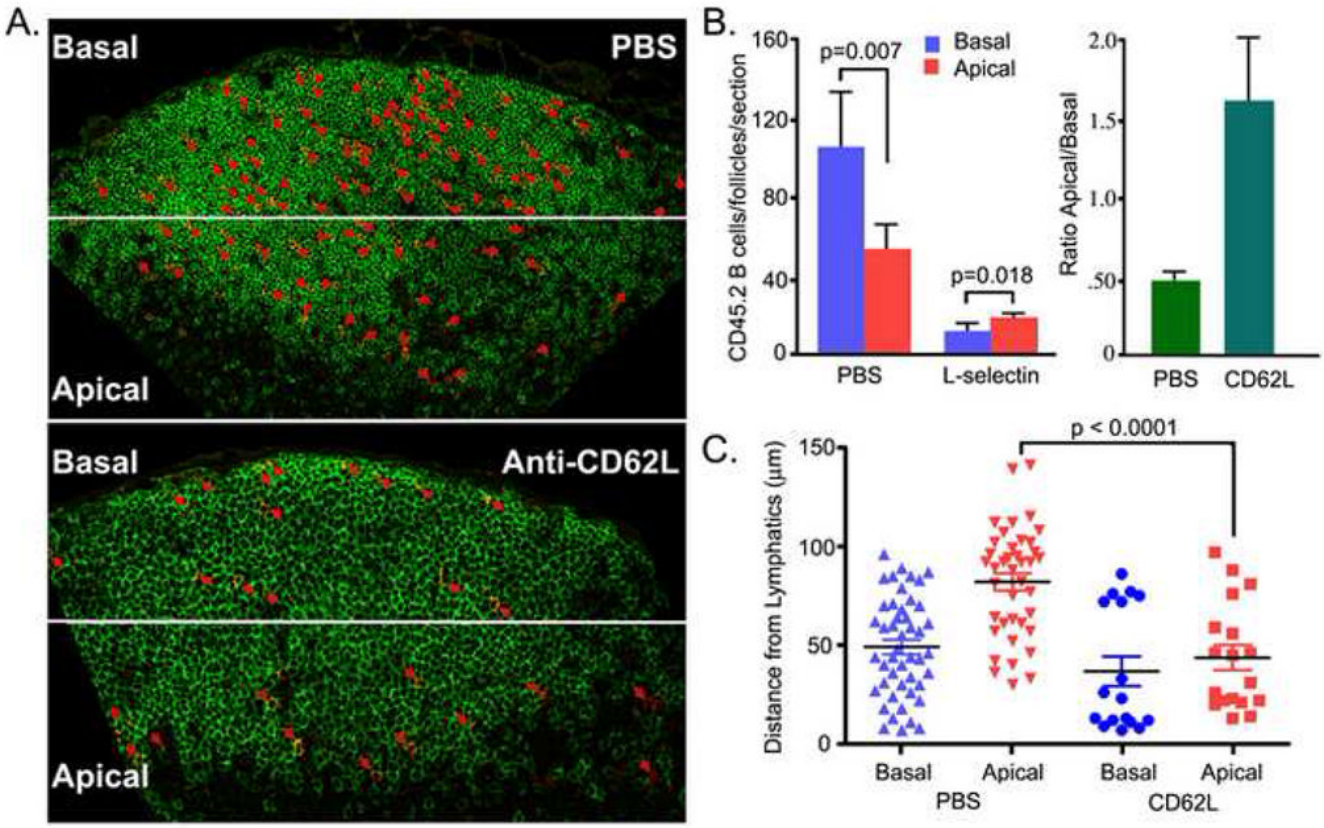

Figure 2.

Relocation of B lymphocytes within the lymph node follicle following blockage of lymphocyte ingress. (A) Location of transferred B cells. Twenty million CD45.2 B lymphocytes were transferred to recipient mice (CD45.1). Two hours later one group of mice (n=3) received 100 μg of CD62L antibody and the other group (n=3) received PBS. Eighteen hours after antibody injection the lymph nodes were harvested and immunostained for B220 and CD45.2. The CD45.2 positive cells are highlighted by red arrows. (B). A relative increase in number of transferred B cells in the apical region following CD62L antibody. The lymph node sections were divided into a basal region away from the lymphatics at the T-B boundary and an apical region close to the lymphatics. The number of CD45.2 B cells enumerated (left panel). The ratio between the numbers of cells in the apical and basal regions is shown (right panel). (C) Distance from lymphatics. The distances of the cells in the basal region from the subcapsular sinus and the distances of the cells in the apical region from the lymphoid cortical sinusoids were measured and plotted for the PBS and CD62L antibody treated mice. The statistical difference is between measured distances of the transferred B cells in the apical region of the inguinal lymph node from PBS versus the CD62L antibody treated mice.

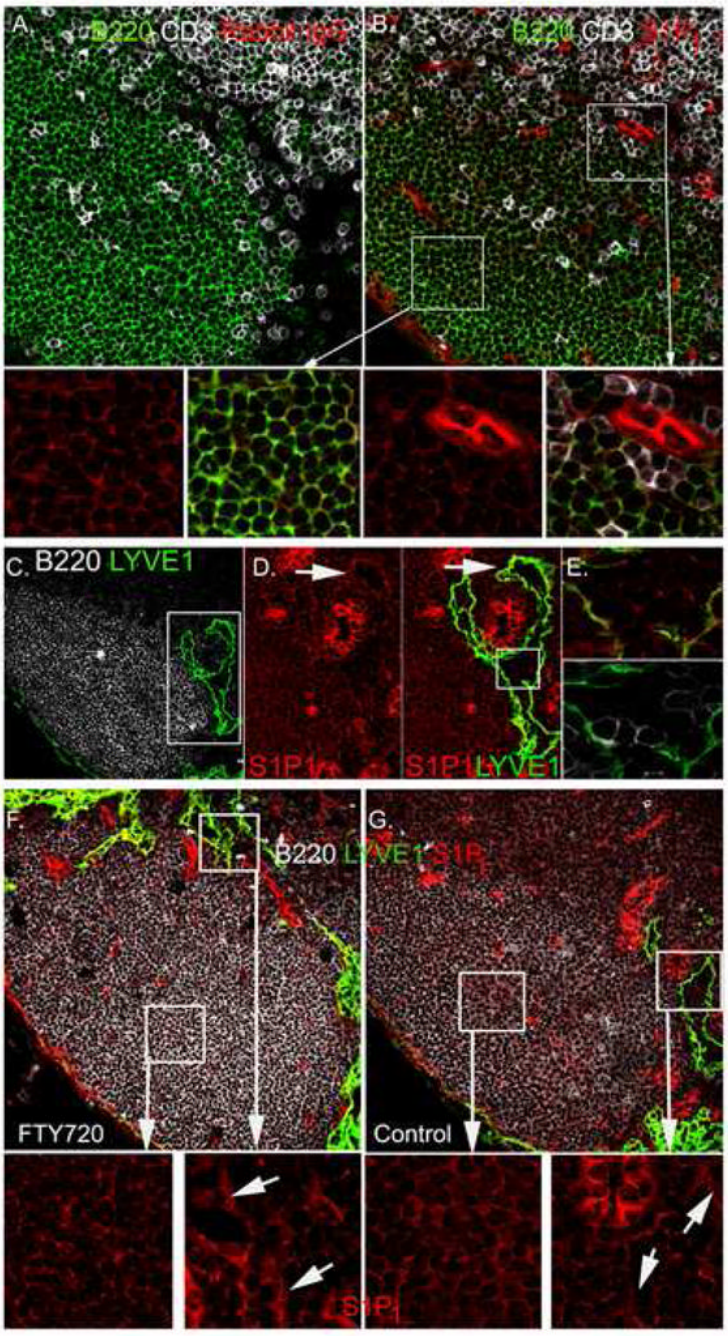

Figure 3.

Location of $S1P_1$ positive B lymphocytes within the lymph node follicle. (A-B) B220, CD3, and $S1P_1$ immunostaining. Lymph node thin sections immunostained as indicated. Rabbit IgG is the control antibody (A) for $S1P_1$ immunostaining (B). Magnified images of the white boxed regions are shown in the lower panels, the left two from deep in the follicle and the right two from the T-B border. (C) B220 and LYVE-1 immunostaining. Lymph node thin section immunostained as indicated. (D) $S1P_1$ and LYVE-1 immunostaining around HEV and lymphatic. The left panel shows $S1P_1$ immunostaining in the region outlined by the white box from part C. Yellow arrows indicate punctate staining of $S1P_1$. The right panel shows $S1P_1$ and LYVE-1 staining of the same region. (E) $S1P_1$ immunostaining of cells in the lymphatics.

Region outlined by white box in part D contains cells within lymphatic lumen. Upper panel shows LYVE- 1 (green) versus S1P1 (red) and lower panel shows LYVE-1 (green) versus B220 (white). (F-G) $S1P_1$ immunostaining of lymph node sections from FTY720 treated and control mice. Mice were treated with FTY720 (1 μg/gm body weight for 18 hours or not). Lymph node sections (7 μM) were stained with antibodies against B220 (white), LYVE-1 (green) and $S1P_1$ (red). White box areas are magnified and $S1P_1$ staining is shown. Lymphatic endothelium staining is indicated (arrows).

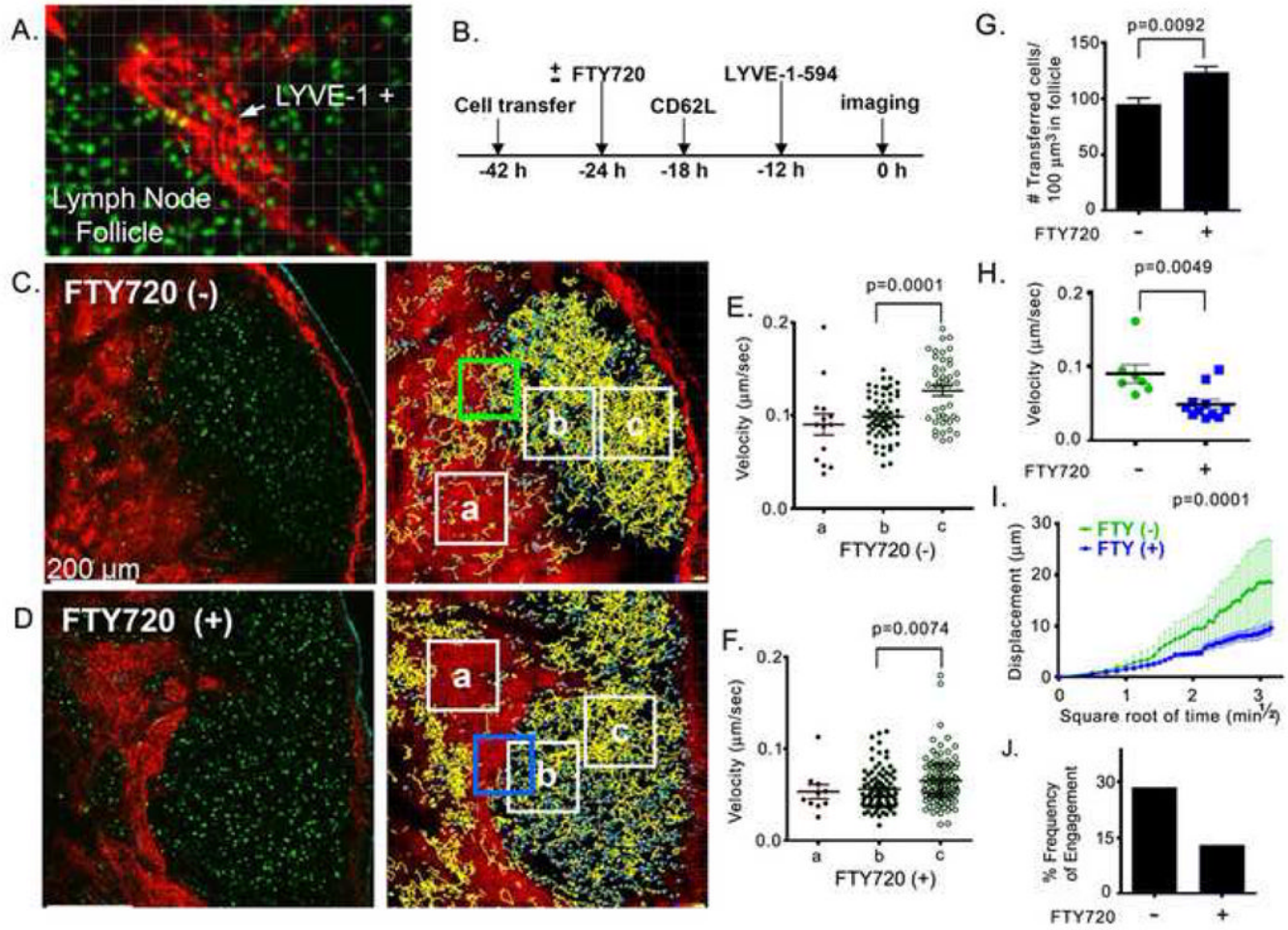

Figure 4.

TP-LSM intravital imaging of LYVE-1 stained structures near the lymph node follicle in the presence or absence of FTY720 (A) Twenty seven µm z-projection of intravital two-photon image stack of inguinal lymph node stained with Alexa Fluor-594 conjugated LYVE-1 antibody to visualize a cortical lymphatic sinusoid (from Supplementary movie 1 online). 10 million CMFDA stained B cells (green) were transferred to the recipient mouse and Alexa Fluor-594 conjugated LYVE-1 antibody (20 µg was injected subcutaneously adjacent to the inguinal lymph node. Lymphatic structures visualized by LYVE-1 antibody are red. (B) Diagram of experiment showing transfer and injection schedule. (C, D) A typical TP-LSM slice from an imaging stack of control and FTY720 treated mice shows LYVE-1 positive signal (red); transferred B cells (green); second harmonics (cyan), (image from Supplementary movies 2 and 3). Scale bar is 200 µm. Right panels show global tracking of adoptively transferred B cells in intact inguinal lymph node. Yellow tracks have an average track speed above the mean of the total and cyan tracks below the mean. Indicated boxes were analyzed below. (E, F) Average speed of adoptively transferred B cells in selected areas (white boxes). The boxes are over the following sites in control and FTY720 treated mice, respectively: a, the LYVE-1 positive region, b, follicle adjacent to LYVE-1 positive region and, c, middle of the follicle. (G) Density of adoptively transferred B cells in B cell follicle. Average number of cells is calculated in 4 different selected areas in B cell follicle from control and FTY720 treated mice. (H) Average speed of selected tracks (control n=7, FTY720 treated n=11) which were coordinated with starting time point in adjacent area to LYVE-1 positive region; green and

blue box in parts C and D, respectively. (I) Mean displacement of selected tracks from part H is plotted versus square root of time. Mean motility coefficient between 0.5 $min^{½}$ and 3.16 $min^{½}$ is 20.57±2.25 um^2/min for control and 2.976 ±0.2753 um^2/min for FTY720 treated. Representative of one of three experiments performed. (J) Frequency at which B cells in the neighborhood of the cortical sinusoids approach the endothelium. B cells within 30 μm of the cortical lymphatic endothelium were manually tracked to determine whether they engaged the endothelium for a minimum of two minutes over a 30 minute imaging span. Data are from representative regions in four separate imaging experiments. 220 cells from FTY720 treated mice and 145 cells from non-treated cells were tracked. % of cells is shown.

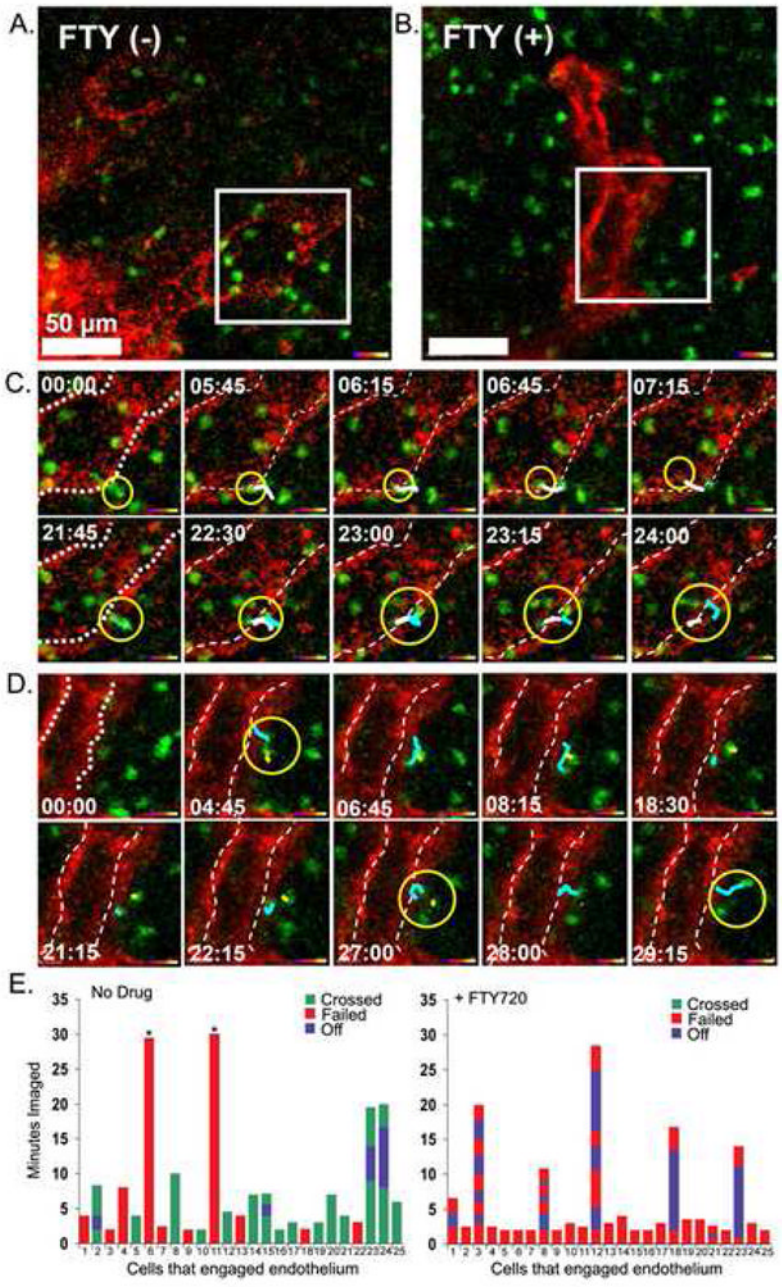

Figure 5.

B lymphocytes migration from the B cell follicle into adjacent lymphatic sinusoids is blocked by FTY720. (A,B) Single slice images (from supplementary movie 4 and 5) with indicated selected area were further analyzed below. Scale bar is 50 um. Similar protocol as was used as in figure 4. Selected white boxes were zoomed. (C,D) Image sequences from white box (from supplementary movie 4 and 5). Delineated lymphatic endothelium marked with doted white line. The yellow circle surrounds three penetrating cells in part C and the yellow circle surrounds two cells unable to penetrate barrier in part D. Time indicator shows the time of the snapshot image from 30 min movies. The dragon tail traces previous 6 time points. Representative of one of three experiments performed. (E) Individual transferred B cells that engaged a cortical lymphatic for a minimum of two minutes were observed during a 30 minute

imaging period. The durations that 25 cells remained associated with the lymphatic endothelium were recorded from intravital TP-LSM imaging experiments performed with either control or FTY720 treated mice. The durations, which cells engaged the endothelium, but failed to cross, are indicated in red, while the durations, which cells engaged and passed, are indicated in green. If a cell disengaged from the endothelium and then re-engaged that duration is indicated in blue. Cells that remained bound to the endothelium for the duration of the imaging are indicated with an asterisk.

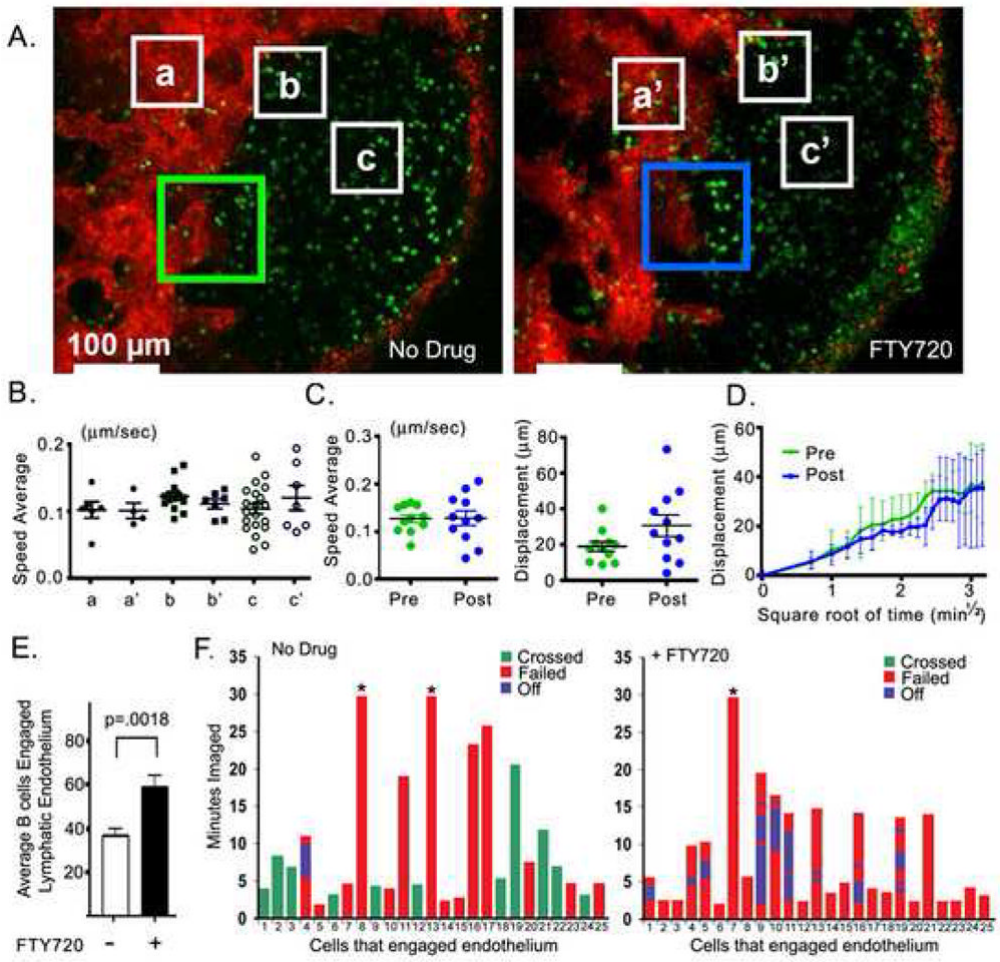

Figure 6.

A four hour treatment of FTY720 does not affect B lymphocyte motility, but prevent B lymphocytes penetration into the lymphatics. (A) Single TP-LSM images (from supplementary movie 6 and 7) with indicated selected areas for further analysis below. 10 million CMFDA stained B cells (green) were transferred to the recipient mouse and 12 hours later Alexa Fluor-594 conjugated LYVE-1 antibody (20 µg) was injected subcutaneously adjacent to the inguinal lymph node. The CD62L antibody was not used. Following an additional 12 hours intravital TP-LSM of the inguinal lymph node was performed after which FTY720 was injected and 4 hours later the same lymph node imaged, Pre (30 min imaging prior to FTY720 treatment) and Post (30 min imaging 4 hours after FTY720 treatment). Boxes (a and a′) represent LYVE-1 positive region; boxes (b and b′) from area adjacent to LYVE-1 positive region; and boxes (c & c′) in the B cell follicle. (B) Average speed average of adoptively transferred B cells in selected areas (white boxes in part A). (C) Average speed and displacement of selected tracks (Pre n=11, Post n=11) in area adjacent to LYVE-1 positive region; green and blue box in part A. (D) Mean displacement of coordinated tracks (Pre n=4, Post n=4) from part C is plotted versus square root of time. Mean motility coefficient between 0.71 $min^{½}$ and 3.16 $min^{½}$ is 36.65±2.827 $µm^2$/min for pre and 36.45 ±2.924 $µm^2$/min for post. (E) Number of cells that engage the lymphatic endothelium. 250 × 250 $µm^2$ TP-LSM images from the same region rich in cortical lymphatics were analyzed for the number of transferred cells found engaged to the lymphatic endothelium at five time points prior to FTY720 treatment and from 5 time points 4 hours after treatment. Average number of cells adherent. (F) Individual transferred B cells

that engaged a cortical lymphatic for a minimum of two minutes were observed during a 30 minute imaging period. The durations that 25 cells remained associated with the lymphatic endothelium were recorded from intravital TP-LSM imaging experiments performed with either control or 4 hour FTY720 treated mice. Analysis is similar to that shown in figure 5E.

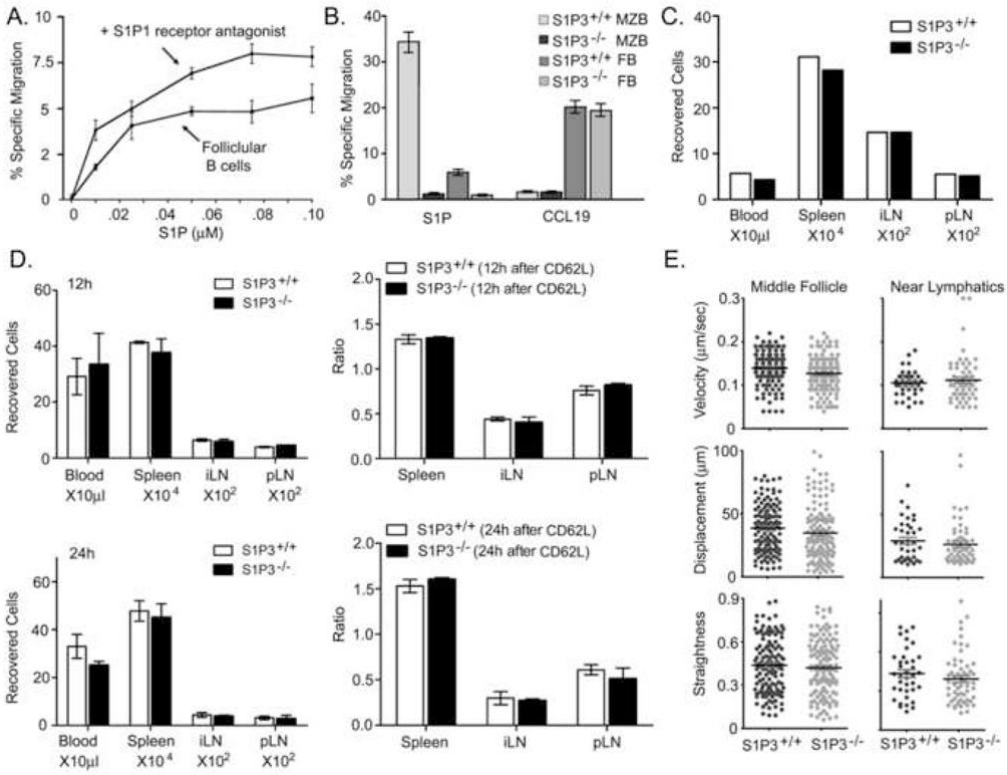

Figure 7.

B lymphocyte lymph node egress does not depend upon S1P mediated chemotaxis. (A). Blocking $S1P_1$ does not inhibit S1P triggered chemotaxis. Chemotaxis of follicular B cells (FB, B220+, CD21 moderate, CD23+) to increasing concentrations of S1P in the presence or absence of VPC23019 (0.5 μM). Data representative of one of 4 experiments performed and is presented as specific migration. (B) $S1P_3$ mediates marginal zone and follicular B cell chemotaxis to S1P. Specific migration of follicular and marginal zone (MZ, B220+, CD21 high, CD23−) B cells from wild type and $S1P_3^{-/-}$ mice to S1P (0.05 μM) and CCL19 (100 ng/ml). Representative of one of three experiments preformed. (C) Homing assay. Equal numbers of labeled wild type and $S1P_3^{-/-}$ mice B cells were intravenously transferred to recipient mice (2 experiments each with 3 pairs of mice). Two hours after transfer, cells from blood, spleen, inguinal lymph nodes, and popliteal lymph nodes of recipient mice were analyzed using flow cytometer. Shown are the actual number of transferred B cells found in blood, spleen, and lymph nodes. (D) Lymph node transit assay. Ten million labeled wild type cells and the same number of labeled $S1P_3^{-/-}$ B cells were intravenously transferred to recipient mice (2 experiments each with 6 pairs of mice). CD62L antibody (100 μg/mouse) was injected intravenously 2 hours after cell transfer to 4 pairs of mice. 2 matched pairs of mice were injected with PBS and the numbers of recovered cells measured. 12 hours (2 pairs) and 24 hours (2 pairs) after antibody injection the cells were also recovered from the indicated sites. The ratios between the cells recovered 12 hours after antibody, 24 hours after antibody, and prior to antibody treatment are shown in the right panels. (E) Motility parameters. Adoptively transferred labeled wild type and $S1P_3^{-/-}$ B cells were imaged by TP-LSM intravitally and tracked over 30 minutes in either the middle of the lymph node follicle or in the region of LYVE-1 positive lymphatics of the inguinal lymph node. Average velocity, displacement, and relative straightness of the tracks are plotted for individual cells. Representative of one of three experiments performed.

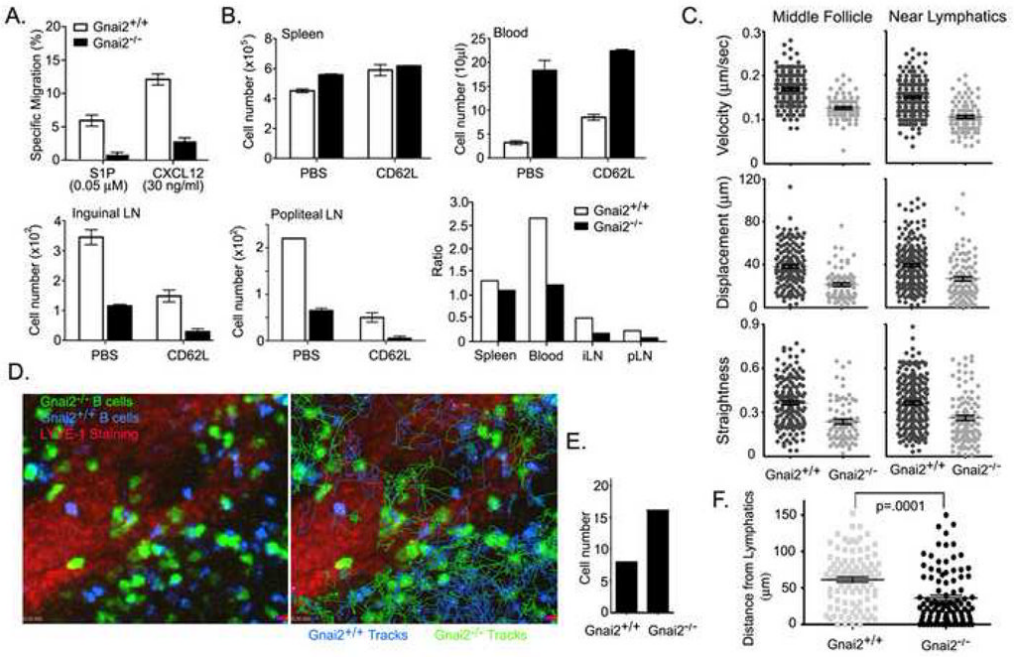

Figure 8. *Gnai2*$^{-/-}$ B cells exhibit reduced S1P and chemokine triggered migration, but rapidly transit lymph nodes

(A) Migration assay. Chemotaxis assay to S1P and CXCL12 using wild type and *Gnai2*$^{-/-}$ B cells (representative of one of 4 experiments performed). (B) Lymph node transit assay. Twelve million labeled wild type cells and the same number of labeled *Gnai2*$^{-/-}$ B cells were intravenously transferred to recipient mice (2 experiments each with 4 pairs of mice). 2 pairs of mice were injected with CD62L antibody (100 μg/mouse) intravenously 2 hours after cell transfer and the number of cells recovered enumerated 18 hours after antibody injection. 2 pairs of mice were injected with PBS 2 hours after transfer and the cells recovered from indicated sites were determined immediately. The ratios between the cells recovered 18 hours antibody treated and prior to antibody treatment are shown in the last panel. (C) Motility parameters. Adoptively transferred labeled wild type (10 million) and *Gnai2*$^{-/-}$ B cells (20 million) were imaged intravitally by TP-LSM in the inguinal lymph node. The cells were tracked over 30 minutes in either the middle of the lymph node follicle or in the region of LYVE-1 positive lymphatics. Average velocity, displacement, and relative straightness of the tracks are plotted for individual cells. (D) Tracks of wild type and *Gnai2*$^{-/-}$ B cells around cortical lymphatics. Left panel shows an image from intravital TP-LSM of wild type and *Gnai2*$^{-/-}$ B in the region of lymphatics of the inguinal lymph node. The right panel shows the same image with superimposed tracks from wild type (blue) and *Gnai2*$^{-/-}$ (green) B cells from 30 minutes of imaging. (E) Cells observed crossing cortical lymphatics. Number of wild type and *Gnai2*$^{-/-}$ B cells observed entering cortical lymphatics. Data combined from 3 separate 30 minute imaging experiments. (F) Localization of cells relative to LYVE-1 positive cortical lymphatics. Imaging spaces 200 × m × 200 μm × 20 μm (x,y,z) were centered around a LYVE-1 positive region and the distance of 100 wild type and 100 *Gnai2*$^{-/-}$ B cells from the lymphatic sinusoid measured at arbitrary time points. Data from 3 separate imaging experiments.